EFFICIENT ONLINE DICTIONARY ADAPTATION AND IMAGE RECONSTRUCTION FOR DYNAMIC MRI

Saiprasad Ravishankar, Brian E. Moore, Raj Rao Nadakuditi, and Jeffrey A. Fessler

Dept. of Electrical Engineering and Computer Science, University of Michigan, Ann Arbor, MI, USA

ABSTRACT

Sparsity-based techniques have yielded promising results for dynamic MRI (dMRI) reconstruction. Data-driven methods involving dictionary learning have become increasingly popular, but they involve expensive computation and memory requirements. We propose a framework for online or time-sequential data-driven reconstruction of dynamic MRI sequences from k-t space measurements recorded by one or more receive coils. The spatiotemporal patches of the underlying image sequence are modeled as sparse in a DIctioNary with lOw-ranK AToms (DINO-KAT), and the proposed method estimates the dictionary, sparse coefficients, and images sequentially and efficiently from the time series of MRI measurements. Our experiments demonstrate the promising performance of our schemes for online dMRI reconstruction from limited data.

***Index Terms*—** Sparse representations, dictionary learning, structured models, low-rank models, inverse problems, online algorithms, machine learning.

1. INTRODUCTION

Magnetic resonance imaging (MRI) is a relatively slow imaging modality because the measurements, which are samples in k-space or Fourier space of the object, are acquired sequentially. There has been much interest in accelerating MRI acquisition by sampling fewer (a.k.a. compressed sensing (CS)) k-space samples. Methods to reconstruct MR images from limited measurements typically assume that the image is sparse in some transform domain or dictionary [1] and optimize problems with sparsity (e.g., ℓ_0 or ℓ_1) regularizers.

Dynamic MRI (dMRI) data are inherently or naturally undersampled because the object is changing as the data is collected. Various techniques have been proposed for reconstructing dynamic MR image sequences from limited (randomly sampled) k-t space measurements [2–4]. Such methods may achieve improved temporal (or spatial) resolution by using more explicit signal models rather than conventional k-space data sharing (where data is pooled in time to make sets of k-space data such as in the form of a Casorati matrix [5], which appears to have sufficient samples), but often at the price of increased computation.

While sparse signal models have been popular [2], alternative models have also been studied for dynamic MRI reconstruction in recent years including low-rank models [5–9]. The popular L+S method [4, 10] models the image sequence as the sum of a low-rank (L) and a sparse (S) component, and jointly estimates the components from k-t space data. The S component may be directly sparse or sparse in a known transform or dictionary. There has also been interest in dictionary learning-based approaches for dMRI reconstruction [11–13], which tend to often involve expensive computation or memory use.

In very recent work [14], we presented a framework for online or time-sequential adaptive reconstruction of dynamic (video) data. Here, we investigate the online adaptive reconstruction of dMRI image sequences from limited k-t space measurements. The spatiotemporal patches of the underlying image sequence are modeled as sparse in a (a priori unknown) DIctioNary with lOw-ranK AToms (DINO-KAT). The dictionary, sparse codes, and images are jointly and sequentially estimated from the sequentially processed k-t space data. This data-driven online approach requires only a portion of the data in memory at a time, greatly reducing memory and computation demands versus conventional iterative methods. The adaptive learning of DINO-KAT also leads to lower reconstruction errors than using an online approach with a fixed DCT dictionary.

2. PROBLEM FORMULATION AND ONLINE ALGORITHM

This section briefly presents the problem formulation and algorithm for online adaptive dMRI reconstruction (cf. [14]). The next section presents numerical experimental results and comparisons.

2.1. Data-Driven Online Reconstruction Problem

Here, we present the formulation for online dMRI reconstruction using a dictionary learning regularizer. Let x^t denote the vectorized version of the 3D array obtained by temporally stacking a small number of J consecutive 2D frames or images. The sequence $\{x^t\}$ is obtained via a sliding window (over time) strategy. The following DINO-KAT-

based image reconstruction problem is solved for each time index t (e.g., $t = 1, 2$, etc.) to estimate each x^t sequentially:

$$(\text{P1}) \left\{ \hat{x}^t, \hat{D}^t, \hat{Z}^t \right\} = \underset{x^t, D^t, Z^t}{\arg \min} \frac{1}{2K_t} \left\| A^t x^t - y^t \right\|_2^2$$

$$+ \frac{\lambda_S}{K_t} \sum_{j=1}^t \rho^{t-j} \left(\sum_{l=1}^M \left\| P_l x^j - D^t z_l^j \right\|_2^2 + \lambda_Z^2 \left\| Z^j \right\|_0 \right)$$

$$\text{s.t. } \left\| z_l^t \right\|_\infty \le L, \text{ rank} \left(R(d_i^t) \right) \le r, \ \left\| d_i^t \right\|_2 = 1 \ \forall i, l,$$
$$Z^j = \hat{Z}^j, \ x^j = \hat{x}^j, \ j < t.$$

Here, A^t is the sensing or measurement operator for the frames in x^t, vector y^t denotes measurements, and j indexes time. For example, in parallel imaging with multiple receiver coils, the measurement operator performs frame-by-frame multiplication by coil sensitivities (i.e., SENSE) followed by (undersampled) Fourier encoding. Operator P_l extracts a vectorized spatiotemporal (3D) patch containing n pixels from x^t. The patches are modeled as sparse in an unknown, adaptive dictionary $D^t \in \mathbb{C}^{n \times m}$ (with columns d_i^t), and $z_l^t \in \mathbb{C}^m$ denotes the coefficients for $P_l x^t$ (i.e., $P_l x^t \approx D^t z_l^t$). Matrix Z^t has z_l^t as its columns for $l = 1, \dots, M$.

The parameter $\lambda_S \ge 0$ controls the overall regularization strength in (P1), and $\lambda_Z \ge 0$ controls overall sparsity of matrix Z^t, where $\left\| Z^t \right\|_0$ counts the total number of non-zeros in Z^t. The operator $R(\cdot)$ reshapes dictionary columns into space-time matrices, which are constrained to have rank at most $r > 0$. Spatiotemporal patches have correlations along time and are well represented in a DINO-KAT model [13]. The ℓ_∞ constraints prevent pathologies that could theoretically arise (e.g. unbounded algorithm iterates) due to the non-coercive objective [13]. In practice, L is set very large, and the constraints are typically inactive.

For each t, we only solve for the latest array x^t and coefficients Z^t in (P1), and previous (older) arrays and coefficients are held fixed, but we adaptively learn D^t using all the patches extracted from the entire sequence $\left\{ x^j \right\}_{j=1}^t$ of 3D arrays. Although D^t is estimated using past information, the proposed algorithm in Section 2.2 does not store this information explicitly; rather, it maintains some sequentially updated (small) matrices to perform the updates. The (exponential) forgetting factor ρ^{t-j} with $0 < \rho < 1$ in (P1) diminishes the influence of old data, and $K_t = \sum_{j=1}^t \rho^{t-j}$ is a normalization constant. The individual frames may occur in multiple (overlapping) windows or arrays x^t. In such cases, we weight the instantaneous estimates from these windows according to the forgetting factors to yield the final frame estimates.

2.2. Algorithm

For each t, our algorithm for (P1) uses a warm start for the dictionary (the previous estimate, $\hat{D}^{t-1}$), sparse codes, and for frames that were estimated in neighboring windows. The algorithm alternates a few times between updating (D^t, Z^t)

(the *dictionary learning step*) and x^t (the *image update step*). We describe these updates in the following.

Minimizing (P1) with respect to (D^t, Z^t), we set $C^t = (Z^t)^H$ to yield:

$$(\text{P2}) \ \min_{D^t, C^t} \sum_{j=1}^t \rho^{t-j} \left\| P^j - D^t (C^j)^H \right\|_F^2 + \lambda_Z^2 \left\| C^t \right\|_0$$

$$\text{s.t. } \left\| c_i^t \right\|_\infty \le L, \text{ rank} \left(R(d_i^t) \right) \le r, \ \left\| d_i^t \right\|_2 = 1 \ \forall i,$$

where P^j is a matrix with columns $P_l x^j$ ($1 \le l \le M$), and c_i^t denotes the ith column of C^t.

Similar to recent work [13], we use a block coordinate descent approach to update c_i^t (i.e., minimize with respect to c_i^t keeping the other variables fixed) followed by d_i^t in (P2), and cycle over all such columns (all i). The exact solution for c_i^t (assuming $L > \lambda_Z$) involves truncated hard-thresholding, and takes the form [13]:

$$\hat{c}_i^t = \min \left(\left| H_{\lambda_Z} \left((E_i^t)^H d_i^t \right) \right|, L1_M \right) \odot e^{j \angle (E_i^t)^H d_i^t}. \quad (1)$$

Here, $E_i^t \triangleq P^t - \sum_{k \neq i} d_k^t (c_k^t)^H$, $H_{\lambda_Z}(\cdot)$ sets vector entries with magnitude $< \lambda_Z$ to zero, 1_M is a length-M vector of ones, "$\odot$" denotes element-wise multiplication, and $e^{j \angle \cdot}$ computes element-wise phase. The solution is based only on the most recent data from (time t) and variable estimates, and is computed cheaply using sparse multiplications (i.e., $(E_i^t)^H d_i^t = (P^t)^H d_i^t - C^t (D^t)^H d_i^t + c_i^t$).

The solution for d_i^t (in (P2)) involves sparse multiplications and a singular value decomposition truncated to rank-r and appropriately normalized [13]. This update makes use of all past patches and sparse coefficients; however, we do not need to explicitly store this past information, rather we recursively (over time) accumulate $P^t C^t$ and $(C^t)^H C^t$ respectively with appropriate forgetting factors into two (small) matrices that we use to compute the optimal d_i^t (cf. [14]).

Minimizing (P1) with respect to x^t yields the simple least squares problem:

$$(\text{P3}) \ \min_{x^t} \frac{1}{2} \left\| A^t x^t - y^t \right\|_2^2 + \lambda_S \sum_{l=1}^M \left\| P_l x^t - D^t z_l^t \right\|_2^2. \quad (2)$$

For single-coil Cartesian MRI, the solution can be obtained using patch-based operations and FFTs [15]. For multiple coil MRI, we use a few iterations of the proximal gradient scheme for (P3) [13, 16, 17].

For each time t, with $m \propto n$, the computations in the above online algorithm are dominated by matrix-vector multiplications, and scale as $O(n^2 M)$. The memory or storage cost scales as $O(nM)$ (assuming $J \ll n$) for storing (only) image patches at time t. Since the number of such patches is typically much smaller than for conventional batch processing algorithms, the online algorithm has a modest memory cost.

Undersampling	4x	8x	12x	16x	20x	24x
NRMSE (Online DINO-KAT) %	**10.2**	**12.9**	**14.8**	**16.6**	**18.3**	**18.1**
NRMSE (Online DCT) %	10.8	13.7	15.8	18.3	20.7	20.8
NRMSE (L+S) %	11.0	13.9	16.1	18.5	21.5	22.5
Gain over Online DCT (dB)	0.5	0.5	0.6	0.8	1.1	1.2
Gain over L+S (dB)	0.7	0.6	0.7	0.9	1.4	1.9

Table 1. NRMSE values as percentages for the cardiac perfusion data for the proposed online DINO-KAT learning-driven method, the online scheme with fixed DCT dictionary, and the L+S method. Results are shown for several undersampling factors with Cartesian sampling. The NRMSE gain (in dB) achieved by the proposed online DINO-KAT learning-driven method over the other methods is also shown.

Undersampling	5x	6x	7x	9x	14x	27x
NRMSE (Online DINO-KAT) %	**9.0**	**9.7**	**11.0**	**12.4**	**15.4**	**20.9**
NRMSE (Online DCT) %	9.5	10.2	11.5	13.2	16.4	22.5
NRMSE (L+S) %	11.9	13.0	14.4	16.6	20.0	25.9
Gain over Online DCT (dB)	0.5	0.4	0.4	0.5	0.5	0.6
Gain over L+S (dB)	2.4	2.5	2.3	2.5	2.3	1.9

Table 2. NRMSE values as percentages for the PINCAT data for the proposed online DINO-KAT learning-driven method, the online scheme with fixed DCT dictionary, and the L+S method. Results are shown for several undersampling factors with pseudo-radial sampling. The NRMSE gain (in dB) achieved by the proposed online DINO-KAT learning-driven method over the other methods is also shown.

3. NUMERICAL EXPERIMENTS

Here, we reconstruct dMRI data from limited measurements using the proposed online reconstruction scheme. We work with the multi-coil (12-element coil array) cardiac perfusion data [4] and the PINCAT data [11, 18] from prior works. For the cardiac perfusion data, we retrospectively undersampled the k-t space using variable-density random Cartesian undersampling (with a different undersampling pattern for each time frame), and for the PINCAT data we used pseudo-radial sampling (with a random rotation of radial lines between frames). We obtained reconstructions at various undersampling factors using the L+S method [4], the proposed online DINO-KAT learning-driven method ($r = 1$), and the proposed online scheme with a fixed DCT dictionary.

For the online schemes, we used $8 \times 8 \times 5$ patches, $\rho = 0.9$, $J = 5$ frames per window, a temporal window stride of 1 frame, and 320×320 dictionaries with atoms reshaped into 64×5 (space-time) matrices. We ran the online scheme for each t for 10 outer iterations (we used 50 outer iterations for the first batch of 5 frames), with 1 and 10 inner iterations in the dictionary learning and image update steps, re-
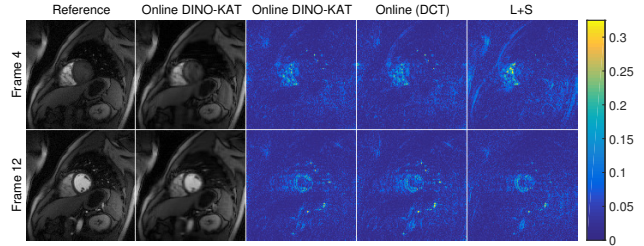
Fig. 1. Two representative frames from a reference (fully sampled) reconstruction of the cardiac perfusion data along with the corresponding frames from the online DINO-KAT learning-based reconstruction from 12x undersampled data (Cartesian sampling). The right three columns depict the corresponding reconstruction error maps (w.r.t. reference) for the online DINO-KAT learning-driven method, the online method with fixed DCT dictionary, and the L+S method, respectively.

spectively. The dictionary and image frames were not updated during the first 3 outer iterations to allow the sparse coefficients to adapt to new patches. The regularization weights for the online schemes were obtained by sweeping over a range of values and selecting values that achieved good reconstruction quality at intermediate undersampling factors. We measured the dMRI reconstruction quality using the normalized root mean square error (NRMSE) metric that is computed as $\|f_{\text{recon}} - f_{\text{ref}}\|_2 / \|f_{\text{ref}}\|_2$, where f_{ref} is a reference reconstruction (from "fully sampled" data), and f_{recon} is the reconstruction from undersampled data. The online schemes were initialized in the first batch with a 320×320 DCT dictionary for D, and the sparse coefficients were initialized with zero. New frames (those not appearing in the preceding window) were initialized by performing zeroth-order interpolation at non-sampled k-t space locations (by inserting the nearest non-zero sampled or reconstructed entry along time) and then backpropagating the filled k-t space to image space by pre-multiplying with the A^H corresponding to fully sampled data.

For the L+S method, we used the publicly available MATLAB implementation [19] with a temporal Fourier transform as the sparsifying transform for the S component. We ran the method for 250 iterations. The remaining parameters for L+S were also selected by sweeping over a range of values and selecting values that achieved good reconstruction quality at intermediate undersampling factors.

Tables 1 and 2 show the reconstruction NRMSE values obtained with the proposed dictionary learning-based online scheme and L+S, along with NRMSE values for the online scheme with a fixed DCT dictionary. The online data-driven approach clearly outperforms the others at various undersampling factors for both the cardiac perfusion data and PINCAT data. Compared to the L+S method [4] that stores and acces-
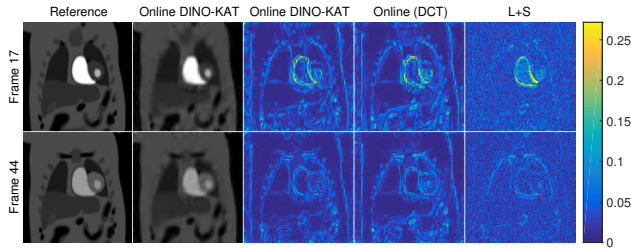
Fig. 2. Two representative frames from a reference (fully sampled) reconstruction of the PINCAT data along with corresponding frames from the online DINO-KAT learning-driven reconstruction from 9x undersampled data (pseudo-radial sampling). The right three columns show the corresponding reconstruction error maps (w.r.t. reference) for the online DINO-KAT learning-driven method, the online method with fixed DCT dictionary, and the L+S method, respectively.
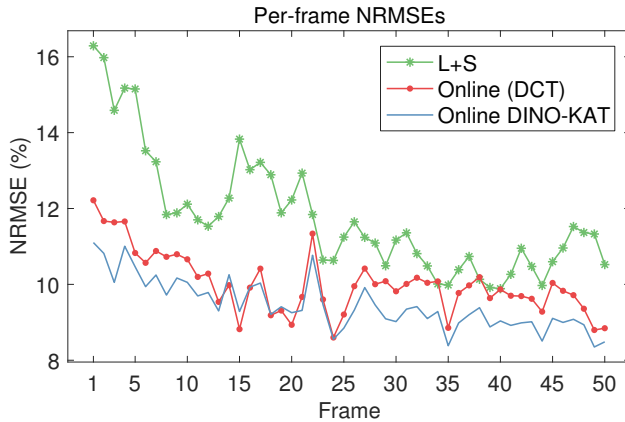
Fig. 3. Per-frame NRMSE values (in percentages) for the L+S method, the online DINO-KAT learning-driven method, and the online method with fixed DCT dictionary, respectively, for the PINCAT data with 5x undersampling (pseudo-radial).

ses all the k-t space data and images in memory during reconstruction, the online scheme only processes/stores data corresponding to 5 frames (in x^t) at any time along with some small (accumulated) matrices. As such, it is well-suited for processing large-scale or streaming data.

Figs. 1 and 2 show reconstructed frames and reconstruction error maps (magnitudes displayed) that illustrate the reduced artifacts achieved with the proposed data-driven scheme. Fig. 3 shows that the online DINO-KAT scheme typically provides better frame-by-frame NRMSE compared to the other methods. Fig. 4 shows time series $(y - t)$ reconstruction plots for the various methods for the PINCAT data. The L+S and online DCT-based methods show line-like or additional smoothing artifacts that are not produced by the proposed online dictionary learning-based scheme.
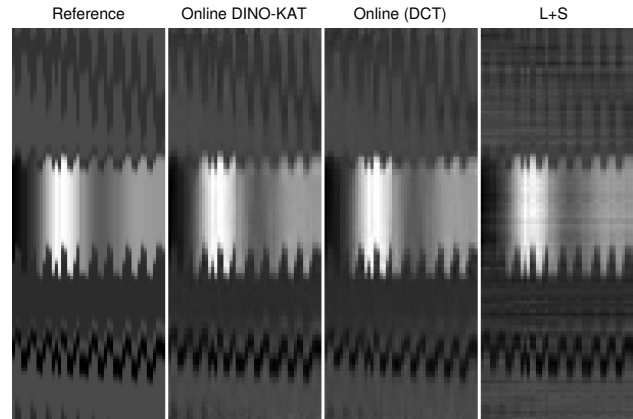
Fig. 4. Temporal $(y - t)$ profiles of a spatial vertical line cross section are shown for the reference PINCAT reconstruction, the online DINO-KAT learning-driven method, the online method with fixed DCT dictionary, and the L+S method for 7x undersampling and pseudo-radial sampling.

4. CONCLUSIONS

We presented a framework for online reconstruction of dynamic MR image sequences by adaptively learning dictionaries with low-rank (reshaped) atoms from sequentially processed k-t space data. The proposed method provides promising performance for dMRI reconstruction from limited data. This work provided an initial exploration of online data-driven methodologies for medical imaging. We plan to explore the promise of the proposed framework in applications such as interventional imaging in future work.

5. ACKNOWLEDGMENTS

6. REFERENCES

[1] M. Lustig, D.L. Donoho, and J.M. Pauly, "Sparse MRI: The application of compressed sensing for rapid MR imaging," *Magnetic Resonance in Medicine*, vol. 58, no. 6, pp. 1182–1195, 2007.

[2] M. Lustig, J. M. Santos, D. L. Donoho, and J. M. Pauly, "k-t SPARSE: High frame rate dynamic MRI exploiting spatio-temporal sparsity," in *Proc. ISMRM*, 2006, p. 2420.

[3] H. Jung, K. Sung, K. S. Nayak, E. Y. Kim, and J. C. Ye, "k-t FOCUSS: A general compressed sensing fra-

mework for high resolution dynamic MRI," *Magnetic Resonance in Medicine*, vol. 61, no. 1, pp. 103–116, 2009.

[4] R. Otazo, E. Candès, and D. K. Sodickson, "Low-rank plus sparse matrix decomposition for accelerated dynamic MRI with separation of background and dynamic components," *Magnetic Resonance in Medicine*, vol. 73, no. 3, pp. 1125–1136, 2015.

[5] Z. P. Liang, "Spatiotemporal imaging with partially separable functions," in *IEEE International Symposium on Biomedical Imaging: From Nano to Macro*, 2007, pp. 988–991.

[6] J. P. Haldar and Z. P. Liang, "Spatiotemporal imaging with partially separable functions: A matrix recovery approach," in *IEEE International Symposium on Biomedical Imaging: From Nano to Macro*, 2010, pp. 716–719.

[7] B. Zhao, J. P. Haldar, C. Brinegar, and Z. P. Liang, "Low rank matrix recovery for real-time cardiac MRI," in *IEEE International Symposium on Biomedical Imaging: From Nano to Macro*, 2010, pp. 996–999.

[8] H. Pedersen, S. Kozerke, S. Ringgaard, K. Nehrke, and W. Y. Kim, "k-t PCA: Temporally constrained k-t BLAST reconstruction using principal component analysis," *Magnetic Resonance in Medicine*, vol. 62, no. 3, pp. 706–716, 2009.

[9] J. Trzasko and A. Manduca, "Local versus global low-rank promotion in dynamic MRI series reconstruction," in *Proc. ISMRM*, 2011, p. 4371.

[10] E. J. Candès, X. Li, Y. Ma, and J. Wright, "Robust principal component analysis?," *J. ACM*, vol. 58, no. 3, pp. 11:1–11:37, 2011.

[11] S. G. Lingala and M. Jacob, "Blind compressive sensing dynamic MRI," *IEEE Transactions on Medical Imaging*, vol. 32, no. 6, pp. 1132–1145, 2013.

[12] J. Caballero, A. N. Price, D. Rueckert, and J. V. Hajnal, "Dictionary learning and time sparsity for dynamic MR data reconstruction," *IEEE Transactions on Medical Imaging*, vol. 33, no. 4, pp. 979–994, 2014.

[13] S. Ravishankar, B. E. Moore, R. R. Nadakuditi, and J. A. Fessler, "Low-rank and adaptive sparse signal (LASSI) models for highly accelerated dynamic imaging," *IEEE Transactions on Medical Imaging*, vol. 36, no. 5, pp. 1116–1128, 2017.

[14] B. E. Moore and S. Ravishankar, "Online data-driven dynamic image restoration using DINO-KAT models," in *IEEE International Conference on Image Processing (ICIP)*, 2017, to appear.

[15] S. Ravishankar and Y. Bresler, "MR image reconstruction from highly undersampled k-space data by dictionary learning," *IEEE Trans. Med. Imag.*, vol. 30, no. 5, pp. 1028–1041, 2011.

[16] P. L. Combettes and V. R. Wajs, "Signal recovery by proximal forward-backward splitting," *Multiscale Modeling & Simulation*, vol. 4, no. 4, pp. 1168–1200, 2005.

[17] N. Parikh and S. Boyd, "Proximal algorithms," *Foundations and Trends in Optimization*, vol. 1, no. 3, pp. 127–239, 2014.

[18] B. Sharif and Y. Bresler, "Adaptive real-time cardiac MRI using paradise: Validation by the physiologically improved NCAT phantom," in *IEEE International Symposium on Biomedical Imaging: From Nano to Macro*, 2007, pp. 1020–1023.

[19] R. Otazo, "L+S reconstruction matlab code," http://cai2r.net/resources/software/ls-reconstruction-matlab-code, 2014, [Online; accessed Mar. 2016].